Automated synthesis of fucoidan enables molecular investigations in marine glycobiology

Conor J. Crawford,[1] Mikkel Schultz-Johansen,[2,3] Phuong Luong,[1,4] Silvia Vidal-Melgosa,[2,3] Jan-Hendrik Hehemann,[2,3] Peter H. Seeberger*[1,4]

[1]Max Planck Institute for Colloids and Interfaces, Am Mühlenberg 1, 14476 Potsdam, Germany. [2]Max Planck Institute for Marine Microbiology, Celsiusstraße 1, 28359, Bremen, Germany. [3]MARUM, Center for Marine Environmental Sciences, University of Bremen, Bremen, Germany. [4]Institute for Chemistry and Biochemistry, Freie Universität Berlin, Arnimallee 22, 14195 Berlin, Germany.

Email: peter.seeberger@mpikg.mpg.de

Abstract

Fucoidan, a sulfated polysaccharide found in algae, occupies a central yet enigmatic role in marine carbon sequestration and exhibits a wide array of bioactivities. However, the inherent molecular diversity and structural complexity of fucoidan hinders precise structure-function studies. To address this, we present a rapid and reproducible automated synthesis method for generating well-defined linear and branched α-fucan oligosaccharides. Our syntheses include oligosaccharides with up to 20 *cis*-glycosidic linkages, diverse branching patterns, and 11 sulfate monoesters. In this study, we showcase the utility of these glycans by (i) characterizing two *endo*-acting fucoidan glycoside hydrolases (GH107), (ii) serving as standards for NMR experiments to confirm suggested structures of algal fucoidans, and (iii) developing a fucoidan microarray. This microarray enabled precise screening of the molecular specificity of four monoclonal antibodies targeting fucoidan. Utilizing the antibody BAM2, identified here for its specificity to α-(1→3)-fucoidans featuring 4-*O*-sulfate esters, we provide evidence that such a fucoidan motif is present in a globally abundant marine diatom, *Thalassiosira weissflogii*. Automated glycan assembly provides a robust platform for accelerating research in marine glycobiology, offering access to fucoidan oligosaccharides with distinct structures, thereby facilitating advancements in our collective understanding of how fucoidan's structure influences its function.

Table of contents

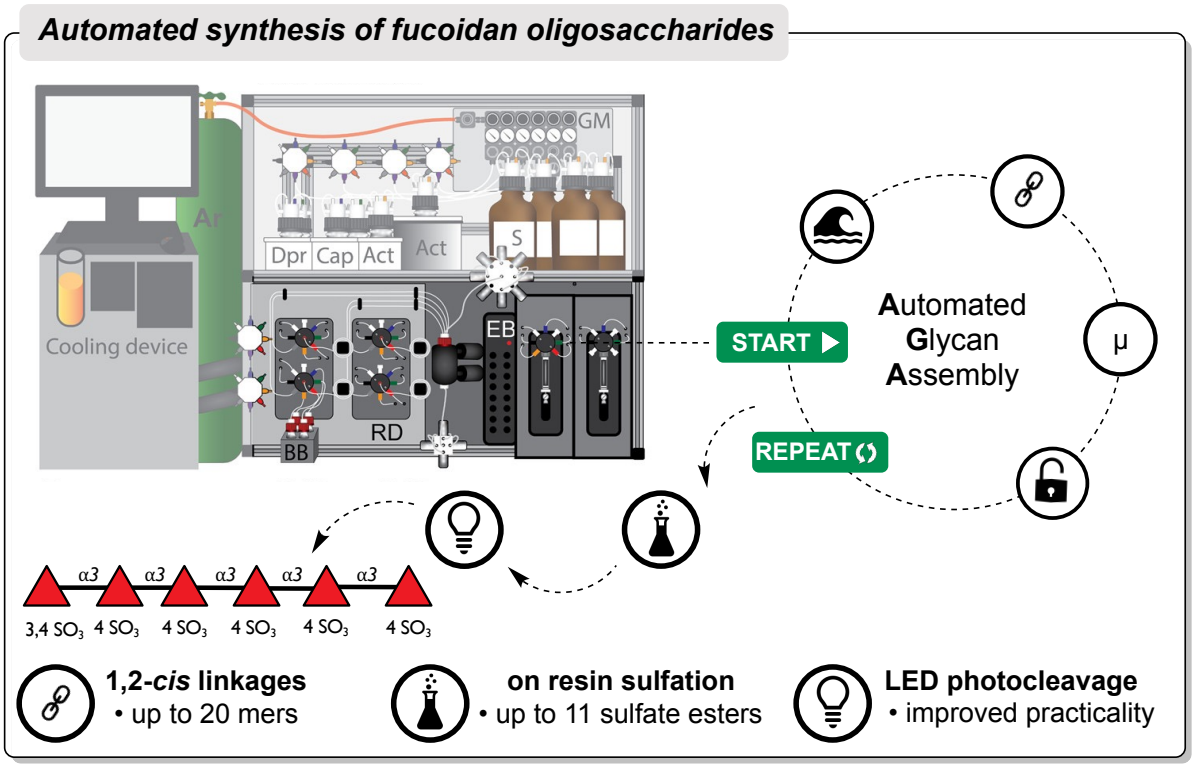

Introduction

Polysaccharides are the central metabolic fuel of the marine carbon cycle. Annually, algae sequester petagrams of carbon dioxide into a rich diversity of glycans.[1] The unique structure of each glycan dictates its residence time and flow within marine ecosystems.[2] Macroalgae and diatoms synthesize and secrete fucose-containing sulfated polysaccharides, termed fucoidan, into the environment.[3,4] The molecular structural diversity of fucoidan poses challenges to marine bacteria, necessitating evolution of equally complex enzymatic cascades for its degradation.[5] Fucoidan that escapes microbial turn-over can self-assemble into particles,[6] sink to the deep ocean and store carbon for centuries.[7,8] Moreover, fucoidan also displays a plethora of biological activities that are under investigation in drug development and cosmetics.[9,10] However, limited knowledge exists regarding the molecular determinants of fucoidan bioactivity or the precise structures within fucoidan responsible for mediating carbon sequestration.

To uncover the molecular mechanisms governing fucoidan carbon sequestration and its bioactivities, well-defined standards are imperative. Extraction from biological systems does not lead to homogenous samples due to the non-template-encoded nature of glycans. Consequently, chemical synthesis stands out as the distinct method to obtain precisely defined organic matter.[11] An automated process would significantly enhance the accessibility of defined fucoidan oligosaccharides. These defined standards would form the basis for a variety of investigations including: creating microarrays,[12–14] delineating the activities of carbohydrate-active enzymes (CAZymes),[15–17] and serving as standards for NMR experiments.[18–20]

The chemical synthesis of complex glycans is challenging,[11] however, advances in automated approaches have enabled high-throughput assembly of both oligosaccharides and polysaccharides.[21,22] The automated chemical synthesis of fucoidan oligosaccharides faces three primary challenges: i) the stereocontrolled formation of 1,2 *cis*-glycosidic bonds,[11,23–27] ii) the high degree of sulfation,[28,29] and iii) the exceptionally high reactivity of glycosyl donors.[30,31]

Here, we present an automated glycan assembly (AGA) process for synthesizing well-defined fucoidan oligosaccharides, encompassing linear α-fucans up to 20-mers, branched fucoidan oligosaccharides, and glycans that contain up to 11 sulfate esters. These glycans served as standards for NMR spectroscopy, aided in delineation of CAZymes activities, and enabled the creation of a fucoidan microarray. Utilizing this microarray, we elucidated the specificity of fucoidan-directed antibodies, which, in turn, led to the discovery that such a glycan motif is synthesized and secreted by the diatom *Thalassiosira weissflogii*.

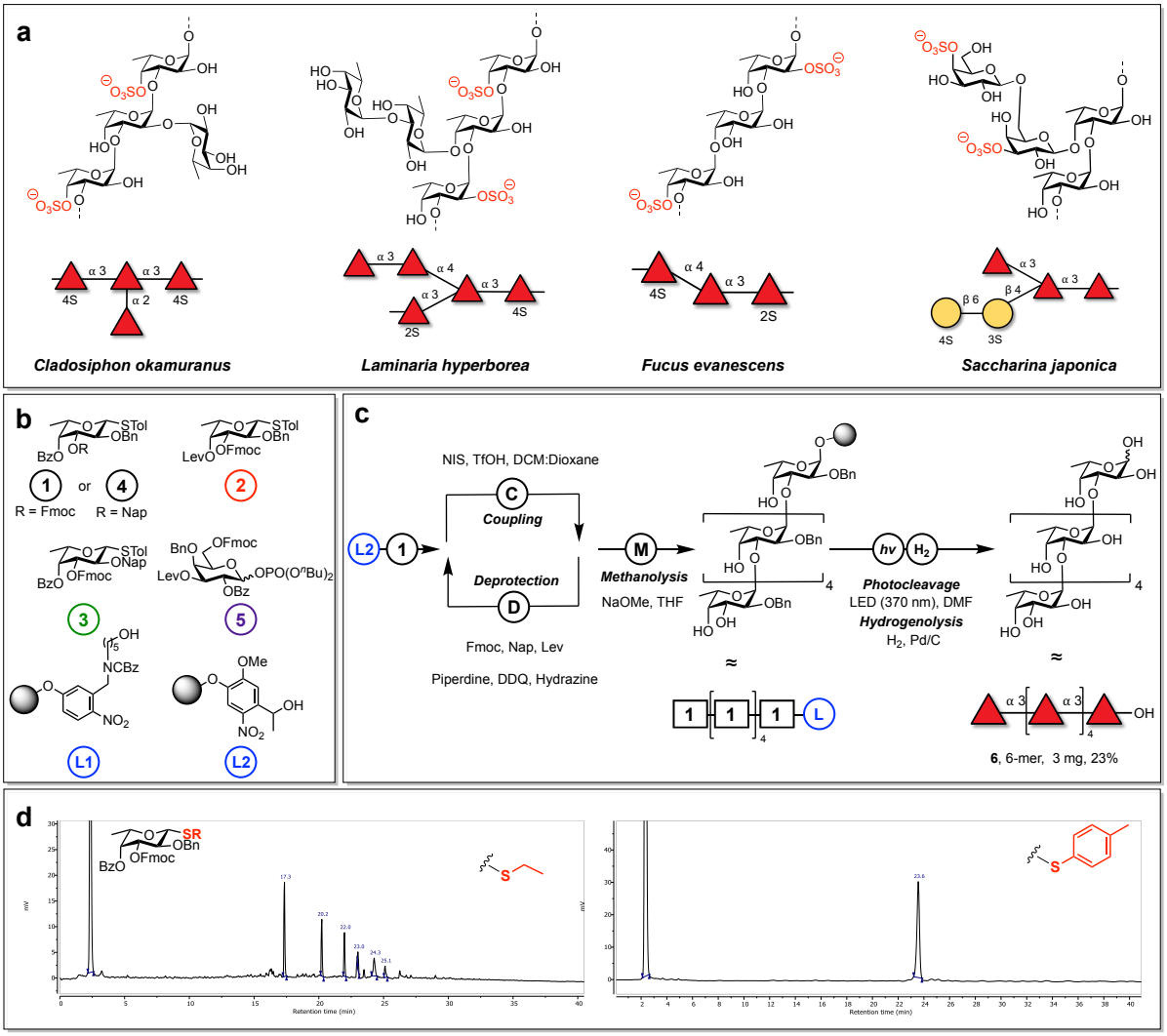

Figure 1. Structural diversity of Fucoidan. a four examples of fucoidan found in brown algae. From Left: *Cladosiphon okamuranus* contains an α-1,3-backbone and is known to possess a degree of 4-*O*-sulfation,[32,33] *Laminaria hyperborea* an α-1,3 linked fucan with a defined number of motifs including those with α-1,4 and α-1,2 branches with sulfate esters primarily on C-2 and C-4,[34] *Fucus evanescens* is an α-1,3/1,4 linked fucoidan,[35] *Saccharina japonica* an α-1,3 linked fucoidan known to contain β-1,4 galactopyranosyl branches.[36] **b** building blocks used in this study. **c** automated assembly of fucoidan

hexasaccharide. **d** Representative example of HPLC traces from AGA of a fucoidan hexasaccharide **6**. Left trace with a thioethyl thioglycoside, right trace with a 4-methylphenyl thioglycoside.

Results and discussion

Retrosynthetic analyses and building block design

Homo- and heterofucans represent two classes of fucoidan. Homofucans consist of either α-(1→3)-linked structures or those with alternating α-(1→3)-α-(1→4)-linked L-fucose linkages. On the other hand, heterofucans do not have a defined glycan backbone and can consist of galactose,[37] mannose or glucuronic acid with fucose branches.[38] The structural diversity of homofucans is expanded by the presence of sulfate esters, acetylation and saccharide modifications like galactose, glucuronic acid or xylose.[32,39] Despite the diverse structures within homofucans across brown algae, each species contains distinct motifs. For instance, fucoidan from *Laminaria hyperborea* primarily features α-(1→3)-linkages, accompanied by smaller quantities of α-(1→2) and α-(1→4)-linkages.[34] Presently, defining precise sulfation patterns in fucoidan polysaccharides is technically challenging. However, *Cladosiphon okamuranus* possess a high degree of 4-*O*-sulfation (**Figure 1a**).[33]

Retrosynthetic analyses identified thioglycoside building blocks **1**–**5** as suitable candidates for assembling different fucoidan oligosaccharides (**Figure 1b**). Building block **1** is equipped with a non-participating benzyl ether on the 2-hydroxyl, a temporary fluorenylmethoxycarbonyl (Fmoc) group on the 3-*O*-position, and the 4-*O*-position was protected with a benzoate ester. The 4-*O*-benzoate ester serves as a long-range participating group (LRP) to support 1,2 *cis*-glycoside formation. Additionally, it can be cleaved on the resin to enable for 4-*O*-sulfation.[40–42] Building block **2** carries a 4-*O*-levulinate ester (Lev) for the formation of 1→4 linkages and could be utilized for precise 4-*O*-sulfation. Building block **3** bears a non-participating 2-naphthylmethyl ether (Nap) protecting group that can be selectively removed to install 1→2 linkages or 2-*O*-sulfate esters. Building block **4**, used a Nap ether at the 3-OH, permitting Lev and Fmoc related protecting group manipulations elsewhere in the oligosaccharide. This Nap ether could later be removed to proceed with the continuation of the backbone synthesis. Finally, building block **5**, allowed for the synthesis of galactopyranoside branches.

Altering the thioglycoside leaving group improves automated glycan assembly of fucoidan oligosaccharides

Initially, thioethyl glycosides were used for AGA of α-(1→3)-homofucans, resulting in significant quantities of deletion sequences and reproducibility problems (**SI Table 1**, **Figure 1c** and **d**, **SI Figure 1**). Efforts to enhance the efficiency of the glycosylation by trialling different Lewis acids, varying temperatures, and employing double coupling cycles, still produced inconsistent results (**SI Table 1,** Entries 1-4). Considering that fucosyl donors are highly reactive,[30,43] and coupling temperatures below -40°C are impossible to adopt at current automated synthesizers,[44] dibutyl glycosyl phosphate donors were tested but did not improve yields (**SI Table 1,** Entries 5 and 6).

Modifying thioglycoside reactivity by changing the protecting groups was impractical due to the structural complexity of the oligosaccharide targets that include branches and sulfate esters. Instead, the thioglycoside aglycon leaving group was modified to regulate glycosyl donor reactivity,[45] which can adjust the activation temperature of thioglycosides by as much as +10°C.[30] Initially, 4-methylthiophenol thioglycosides were chosen for their availability and low cost, enhancing both the quality and reproducibility of the glycosylation modules during AGA. Notably, no deletion sequences were detected by HPLC or MALDI-MS analysis (**Figure 1d** and **SI Figure 1, SI Table 1**, Entries 7 and 8). The optimized glycosylation modules involved *N*-iodosuccinimide (NIS) and triflic acid (TfOH) with a reaction sequence of −20°C for 15 min, followed by 0°C for 35 min using five equivalents of donor.

After improving AGA with 4-methylphenyl thioglycosides, subsequent investigations focused on assessing the stereoselectivity of glycosylations, on-resin methanolysis, photocleavage, sulfation and hydrogenolysis.

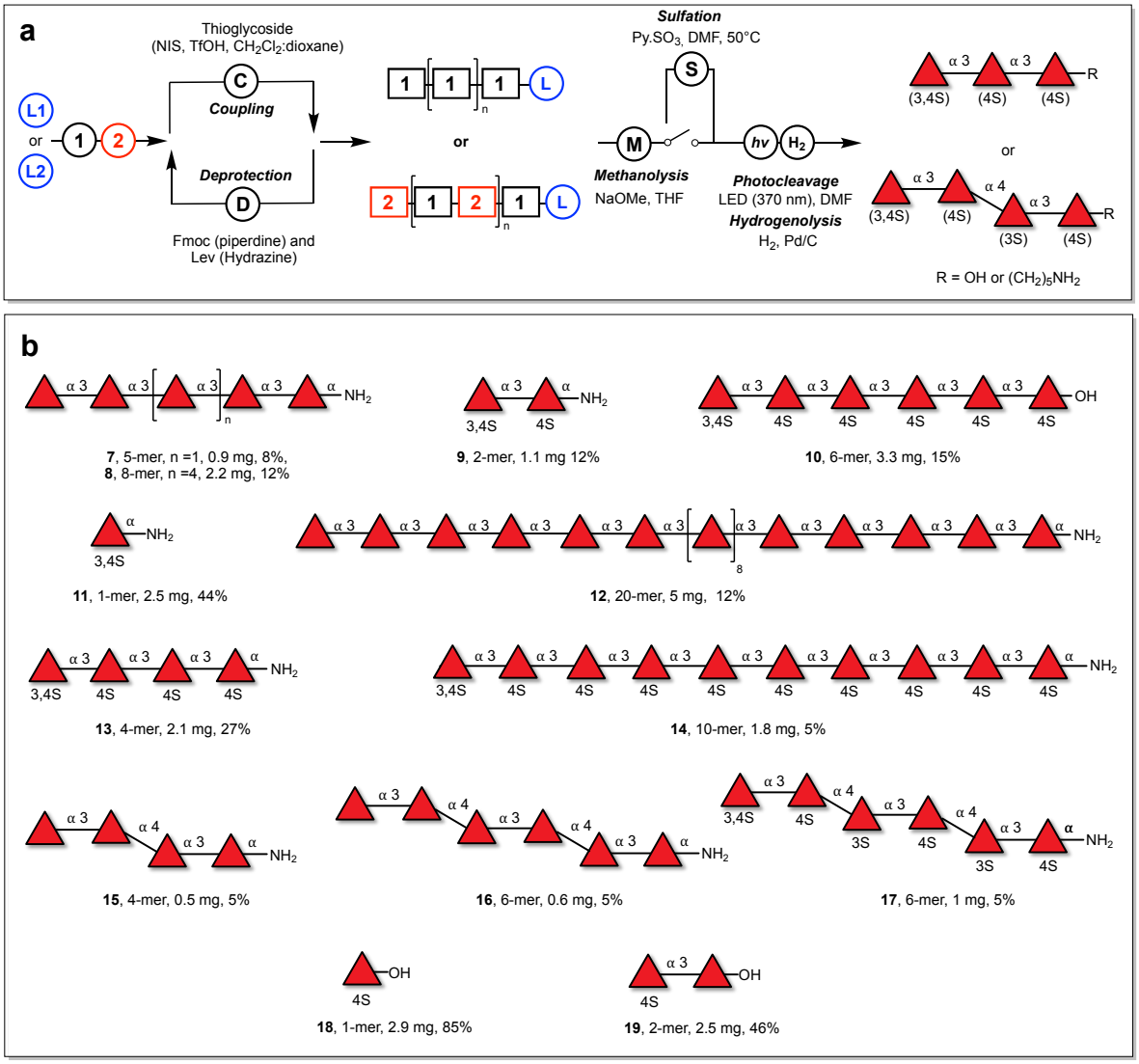

Figure 2. Automated glycan assembly of two major types of fucoidan backbone. a Automated assembly of two types of fucoidan backbone, α-1,3-linked structures and those with alternating α-1,3/α-1,4-linked L-fucose linkages. **b** collection of fucoidan oligosaccharides synthesized.

Automated synthesis of fucoidan oligo- and polysaccharides

The chemical synthesis of 1,2-*cis* glycosides in a stereocontrolled fashion is not a generally solved problem.[11,23–27] However, long-range remote assistance is useful for the synthesis of 1,2-*cis* glucosides and fucosides.[40,41] Leveraging optimised AGA conditions, a series of α-(1→3)-linked fucoidan oligosaccharides, pentamer **7**, hexamer **10**, octamer **8** and a 20-mer **12** were prepared (**Figure 2**).

Polystyrene resins were either equipped with a 5-aminopentanol to release glycans with a terminal amine for coupling to microarray surfaces, or a 'traceless' photocleavable linker,[46] which permits the synthesis of free-reducing end glycosides for enzyme assays.[47] Each coupling cycle consisted of an acidic wash with trimethylsilyl trifluoromethanesulfonate (TMSOTf), followed by NIS-TfOH promoted glycosylation. Subsequently, the resin underwent incubation with a solution of acetic anhydride (Ac_2O) and methanesulfonic acid (MsOH) to 'cap' any unreacted nucleophile (**Figure 2a**).[48] For α-(1→3)-linked fucans, the temporary Fmoc protective group was removed using a piperidine solution (20% in dimethylformamide) to expose the nucleophile for the subsequent coupling cycle. The coupling cycles were reiterated five times for **6**, six times for **10**, and eight times for **8**.

For the synthesis of the 20-mer fucan **12**, an initial assembly of a 10-mer was undertaken, monitoring the process by cleaving and analyzing a small resin sample via MALDI-MS and analytical HPLC (**SI Figure 2a**). Subsequently, the synthesis continued to reach the targeted 20-mer (**SI Figure 2b** and **2c**). Notably, this α-fucan 20-mer **12** matches the length of the largest 1,2-*cis* linked oligosaccharides synthesized by AGA to-date.[22]

The second major backbone of fucoidan comprises alternating α-fucopyranosyl-(1→3)-α-fucopyranosyl-(1→4) linkages. AGA of these oligosaccharides relied on the iterative use of building blocks **1** and **2**, leading to the production of tetramer **15** and hexamer **16**. During the synthesis of these mixed linkage oligosaccharides, the Fmoc protecting group removal module was completed using a 20% triethylamine solution in dimethylformamide. This method was chosen as Lev esters can be sensitive to the treatment with piperidine.[22] Smooth coupling between the axial 4-OH acceptor and thioglycoside **1** was observed without any reactivity issues (**SI Figure 3**).

The methanolysis module, employed for removing base-labile protecting groups, proved ineffective under standard conditions, even after extended incubation periods of 168 hours (10% 0.5M NaOMe in anhydrous THF, 5 mL, v/v).[29,49] However, utilizing a reduced volume (<5%) of sodium methoxide was necessary for efficiently removing the benzoate esters in under 16 hours. Oligosaccharides larger than 10-mers necessitated prolonged incubation periods of 70 hours.

Oligosaccharides **6** and **16** were liberated from the solid support using a flow-based photo-reactor,[50] followed by hydrogenolysis using 5% Pd/C in THF:t-BuOH:H_2O (60:10:30, v/v/v).[51] The two distinct fucoidan backbones were individually purified via reverse-phase HPLC (Hypercarb, gradient 0 to 80%, acetonitrile:water) to yield hexasaccharides **6** and **16**.

NMR analysis confirmed that both fucoidan backbones were prepared with complete α-selectivity, where the only observed β-linkage was associated with the free-reducing end at 4.57 ppm (d, J = 7.9 Hz) in **6**. Comparison of the synthetic fucoidan oligosaccharide NMR spectra to polysaccharides extracted from brown algae showed excellent agreement.[34] Fucoidan oligosaccharides with α-1,3-backbone shifts occurred at ≈ 5.06 ppm (^{1}H NMR) and 95.5 ppm (^{13}C NMR), while the α-1,4-backbone occurred at ≈ 4.96 ppm (^{1}H NMR) and 100.2 ppm (^{13}C NMR).[34] The use of the nucleophilic 5-aminopentanol-linker does not always guarantee high α-selectivity.[52] However, compounds **7**, **8**, **9**, **11**-**17** exhibited only the desired 1,2-*cis* linkage observed in NMR, distinctly presenting an α-linked anomeric proton at ≈ 4.88 ppm (^{1}H NMR) and > 98.2 ppm (^{13}C NMR).

Automated assembly of sulfated fucoidan oligosaccharides

The precise pattern and degree of fucoidan sulfation depends on a range of factors, including environmental conditions, growth stages, and extraction methods. Moreover, our understanding of how different sulfation patterns impact fucoidan's biological functions remains limited. This is in contrast to glycosaminoglycans (GAGs), where well-defined oligosaccharides have played a pivotal role, allowing for a detailed molecular-level understanding of the roles that individual sulfate groups play in modulating bioactivity.[53–55]

The largest sulfated oligosaccharides prepared via AGA to date contain four sulfate esters.[28,29] However, to decode glycan-protein interactions with high fidelity, sulfated tetra- to dodecasaccharides are ideal. Therefore, we initially targeted the synthesis of tetrasaccharide **13** with five sulfate esters. AGA, followed by methanolysis, provided the tetrasaccharide attached to the solid support. Two methods reported for on-resin sulfation failed to achieve full sulfation to the desired penta-*O*-sulfated compound (**Figure 3**, **Table 1**, Entries 1-4, **SI Figure 4**).[29,44] The low nucleophilicity of the axial C4 hydroxyl group and/or the steric demands involved in placing numerous sulfate esters in close proximity on the solid support may be responsible for the observed outcome.

Solution-phase syntheses of sulfated glycans, such as GAGs, often necessitate prolonged reaction times,[42,53] that in turn render sulfation on the instrument not always practical (**Table 1**, Entries 1 and 2).[44] While, a recently published 'off-machine' on-resin approach, conducted in plastic syringes could not provide the precise atmospheric and temperature control necessary for extended reaction times (**Table 1**, Entry 3). Sealable silanized microwave vials proved ideal for carrying out long sulfation reactions in an aluminum heating block (**SI Figure 16**, **Table 1**, Entries 4-7).

In sealed microwave vials both sulfur trioxide pyridine ($Py{\cdot}SO_3$) and triethylamine ($NEt_3{\cdot}SO_3$) complexes yielded comparable results (**Table 1**, Entries 4-5). Pre-buffering the sulfation solution with an appropriate base,[56] such as pyridine for sulfation reactions using $Py{\cdot}SO_3$ helped to minimize batch-to-batch variability in the quality of sulfur trioxide reagents (**Table 1**, Entries 6-7).[57]

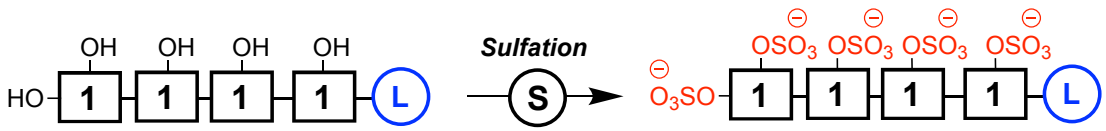

Figure 3. Optimization of on-resin sulfation using tetrasaccharide 13.

Table 1. On resin sulfation optimization.

Entry	Solvent	Reagent	Temperature	Time	Comment	Reference
1.	DMF	$NMe_3 \cdot SO_3$	90°C	30 min (2 cycles)	Incomplete	[44]
2.	DMF	$NMe_3 \cdot SO_3$	90°C	90 min (6 cycles)	Incomplete	[44]
3.	DMF:Py (1:1)	$Py \cdot SO_3$	40°C	12 h	Incomplete	[29]
4.	DMF	$Py \cdot SO_3$	50 °C	16 h	Irreproducible	This work
5.	DMF	$NEt_3 \cdot SO_3$	50°C	16 h	Irreproducible	This work
6.	DMF:Py (80:20)	$Py \cdot SO_3$	50 °C	16 h	Complete	This work
7.	DMF:NEt_3 (80:20)	$NEt_3 \cdot SO_3$	50°C	16 h	Complete	This work

Tracking sulfation reactions on solid-phase is challenging due to a lack of analytic techniques. To monitor sulfation reactions, microcleavage must be performed, which releases minute quantities of oligosaccharides for HPLC and MS analysis. Here, we employed dimethylformamide (DMF) as a photocleavage solvent, which ensured better resin-swelling and solubility of the released sulfated glycans,[58,59] compared to the reported DCM/methanol mixtures.[29] The glycans were analyzed using quadrupole time-of-flight mass spectrometry (Q-TOF MS, **SI Figure 5**) and reverse-phase HPLC (C5 Luna, 5% ACN to 100), with the HPLC analysis only effective for oligosaccharides with fewer than six sulfate esters (**SI Figure 4**).

Using optimized conditions (see SI, modules h1 and h2), solid-phase sulfation from mono- to a decasaccharide was completed (**9-11**, **13**, **14** and **17**). Notably, decasaccharide **14** contained eleven sulfate esters representing the most sulfated biomolecule prepared via solid-phase synthesis to date. To prepare glycans **18** and

19 with precise 4-*O*-sulfation patterns, Lev esters were employed. These esters could be selectively removed using hydrazine, followed by sulfation of the exposed hydroxyl groups. Subsequently, methanolysis cleaved the remaining esters (**Figure 2b**).

Photocleavage using a LED lamp allows for parallel cleavage of multiple resins

Reported approaches for cleaving sulfated oligosaccharides from the solid support involve a mercury lamp flow-reactor set-up, utilizing a DCM-methanol mixture.[29,50] Multiple passages through the flow cell are required to achieve good material recovery,[50] due to poor resin-swelling properties of methanol.[29,50] Similar results were obtained when cleaving sulfated oligosaccharide **10** from the solid support using photolysis. Therefore, we alternatively employed a LED lamp (370 nm) with DMF as a photocleavage solvent.[60,61] DMF was chosen as it can solubilize the released amphiphilic sulfated glycans due and for its good resin-swelling properties.[58,59] The batch reactor facilitated the parallel cleavage of multiple resins (**SI Figure 6**).

Following the release of the oligosaccharides from the solid support, the crude material was subjected to hydrogenolysis (5% Pd/C, THF:t-BuOH: H_2O, 50:20:30, v/v/v), and the sulfated glycans were purified using RP-HPLC, size-exclusion chromatography, or a combination of both methods. The choice of purification method depended on the number of sulfate esters on the oligosaccharide. Glycans containing more than five sulfate esters were best purified using a combination of size-exclusion chromatography and HPLC. Using this approach a series of sulfated fucans (**9**, **10**, **11**, **13**, **14**, and **17**) with different backbones, lengths, and sulfation patterns was prepared (**Figure 2b**).

Automated assembly of branched fucoidan oligosaccharides

Brown algae synthesize a diverse range of fucoidans with distinct branching and sulfation patterns. The utility of the AGA platform to synthesize such branched fucoidans was demonstrated with four examples. These glycans contain α and β branching residues and cover all the theoretical branching patterns found in fucoidan (2-OH, 3-OH, 4-OH).

α-(1→2)-fucopyranoside branches occur in various brown algae species, including *Cladosiphon okamuranus* and *Laminaria hyperborea* (**Figure 1a**). Therefore, we prepared hexasaccharide **20** that contains this motif (**Figure 4a**).[39] Notably, two cycles of building block **3** were required to fully convert the acceptor trisaccharide to the desired tetrasaccharide (**SI Figure 11**), suggesting the glycosyl donor containing a 2-naphthylmethyl ether was less effective under these specific glycosylation conditions. Selective oxidative cleavage of the Nap group facilitated regioselective glycosylation of the 2-OH acceptor (**SI Figure 12**). Subsequently, the Fmoc removal and glycosylation produced the desired protected oligosaccharide intermediate, with HPLC displaying a major peak at 20 minutes (**SI Figure 13**). Following methanolysis, the presence of the semi-deprotected hexasaccharide was confirmed by MALDI-TOF (**SI Figure 14**). Photocleavage released the oligosaccharide from the resin, following hydrogenolysis and HPLC purification 1.6 mg (10%) of α-fucan **20** was isolated. NMR analysis of **20** revealed a distinct up-field chemical shift at 5.33 ppm (d, J = 3.8 Hz, 1H), previously annotated for α-(1→2)-linkages in *Laminaria hyperborea*,[34] therefore, the synthetic oligosaccharide supported the assigned structure.

Subsequently, two *Saccharina japonica* motifs were synthesized, one featuring a β-(1→4)-galactopyranoside branch, and the other presenting a more extended gal-β-(1→6)-gal-β-(1→4) branching pattern.[62] AGA of pentasaccharide **21** relied on building blocks **1** and **2** to construct the tetrasaccharide backbone (**Figure 4b**). Following the removal of the Lev ester, selective galactosylation was completed using the dibutyl phosphate donor **5** (TMSOTf, -35°C for 5 min → -20°C for 30 min, 5.5 equivalents).[63] HPLC analysis revealed a major peak at 32 min for the pentasaccharide (**SI Figure 9**). To assemble glycan **22** with the gal-β-(1→6)-gal-β-(1→4)-branch**,** AGA utilized building blocks **1** and **2**, alongside **4**, containing a 3-Nap ether, permitting future extension of the fucan backbone following the assembly of the galactose chain (**Figure**

4c). HPLC analysis of the hexasaccharide displayed a major peak at 30.52 min (**SI Figure 10**). Following methanolysis, photocleavage, hydrogenolysis and HPLC purification yielded glycans **21** (0.9 mg, 8%) and **22** (0.5 mg, 4%). NMR analysis of **21** showed a β-(1,4)-linkage at 4.52 ppm (d, *J* = 7.3 Hz, 1H), while **22** contained an additional β-linkage at 4.32 ppm

Heptasaccharide **23** contains an α-(1→4)-fucopyranosyl branch found in *Laminaria hyperborea* (**Figure 1a, Figure 4d**).[34] This oligosaccharide was assembled using building blocks **1** and **2**, with the Lev ester on **2** facilitating the synthesis of the α-(1→4)-branch. Microcleavage analysis at the pentasaccharide stage revealed a single major peak at 22.2 min in the HPLC (**SI Figure 7**). Subsequently, the two Fmoc protecting groups were removed, and two coupling cycles of **1** produced the protected branched oligosaccharide (**SI Figure 8**). Methanolysis prior to photolytic release from the solid-phase was followed by hydrogenolysis. Reverse-phase HPLC (Hypercarb, 0 to 80 H_2O) yielded 1.5 mg (10%) of the α-(1→4)-containing fucan **23**. NMR analysis of **23** revealed exclusively 1,2-*cis*-linkages, with the anomeric carbon of the α-(1,4)-linkage occurring at 5.15 ppm (d, *J* = 3.9 Hz, 1H), downfield of the α-(1,3)-linkages.[34]

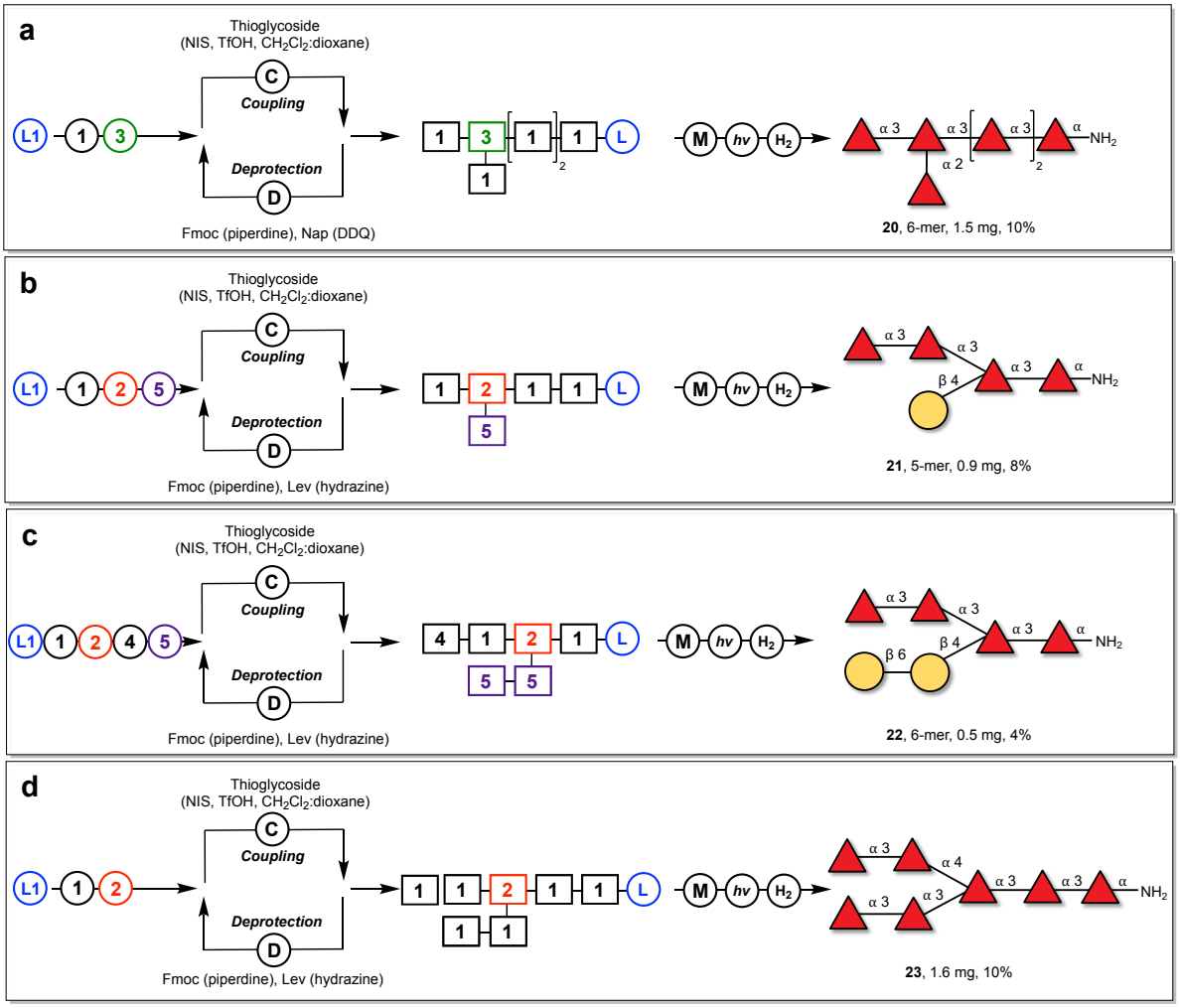

Figure 4. AGA of branched fucoidan oligosaccharides. a synthesis of oligosaccharide **20** with a α-(1→2)-branch found in *Fucus vesiculosus*. **b** synthesis of an oligosaccharide **21** with a β-(1→4)-galactopyranoside branch found in *Saccharina japonica*. **c** synthesis of oligosaccharide **22** with a β-(1→6)-gal-β-(1→4)-galactopyranoside found in *Saccharina japonica*. **d** synthesis of oligosaccharide **23** with a α-(1→4)-branch found in *Laminaria hyperborea*.

Synthetic glycan defines the activity of two *endo*-fucoidan hydrolases

The microbial degradation of fucoidan involves hundreds of enzymes.[5,64] Enhancing our understanding of fucoidan-active CAZymes and their substrate tolerances will advance our mechanistic understanding of how certain fucoidan structures resist degradation, thus facilitating carbon sequestration. Furthermore, characterized enzymes can serve as biocatalytic assays to assist in the detection and quantification of fucoidan in the environment.[65,66]

CAZymes of the glycoside hydrolase family 107 (GH107) cleave in mid-chain glycosidic bonds of algal fucoidans.[67] All current GH107 members are *endo*-fucoidanases targeting either α-1,3 or α-1,4 fucosyl linkages. Several α-1,4-*endo*-fucoidanases have been functionally validated e.g. MfFcnA from *Mariniflexile fucanivorans* and Mef1 from *Allomuricauda eckloniae* for which also protein structures were obtained.[68,69] On the other hand, only one α-1,3-*endo*-fucoidanase has been characterized.[70]

GH107_P5AFcnA from *Psychromonas* sp. SW5A displays activity against fucoidan from *Laminaria hyperborea* – a fucoidan consisting predominantly of sulfated α-1,3-linked fucan – while it is inactive on fucoidans with alternating α-1,3/α-1,4-linked fucan backbone.[34,68] This suggests that GH107_P5AFcnA is an α-1,3-endo-fucoidanase but requires functional validation. Therefore, we used the synthetic α-(1→3) fucan oligosaccharide **10** to test the activity of GH107_P5AFcnA. Recombinant, purified GH107_P5AFcnA was obtained as previously described[68] and the enzyme was incubated with fucoidan and oligo **10**. Enzyme activity and product formation was assayed over time by CPAGE (**Figure 5b**). The results show that GH107_P5AFcnA degrades both fucoidan from *L. hyperborea* as well as oligo **10** and thereby confirms that the enzyme cleaves α-1,3-linked sulfated fucan. Next, we used the protein sequence of GH107_P5AFcnA to search for homolog enzymes at NCBI. A putative GH107 (WP_179351272) from the marine flavobacterium *Winogradskyella vidalii* showed 59% identity (>90% coverage) with GH107_P5AFcnA. Genomic studies have linked *Winogradskyella spp.* to fucoidan utilization, but so far this has not been biochemically verified.[71] We found that pure recombinant GH107 from *W. vidalii* displayed similar activity as GH107_P5AFcnA against fucoidan and α-1,3-linked sulfated fucan oligosaccharide (**Figure 5c**). As such, both enzymes are α-1,3-*endo*-

fucoidanases that are able to initiate the degradation of fucoidan derived from *L. hyperborea*.

According to the CPAGE results, both GH107s show activity against fucoidan after 1 hour, whereas longer incubation time is needed to degrade the oligosaccharide. This suggests that the enzymes prefer substrates with longer glycan chains or different sulfation pattern than **10** – structures that seem to occur in the native fucoidan. For example, fucoidan from *L. hyperborea* can be C2 sulfated in addition to C4.[34] Nevertheless, we demonstrate here the α-(1→3)-fucan specificity of two GH107 fucoidanases derived from marine bacteria. These results demonstrate the utility of synthetic oligosaccharides in discovery and characterization of fucoidan-degrading enzymes.

Glycan microarrays map specificity of fucoidan-directed antibodies

Understanding the relationship between the structure of fucoidans and their functional properties is currently challenging due to the heterogeneity of polysaccharides extracted from algae. Therefore, we constructed a glycan microarray to investigate protein binding to our synthetic fucoidan library. Selected amine-functionalized fucoidan oligosaccharides (**7**, **8**, **9**, **11**, **13**, **20**, and **22**), along with a control β-(1→3)-glucan **24**, were covalently attached to *N*-hydroxylsuccinimide (NHS)-functionalized glass slides. Each glycan was printed in quadruplicate at the concentration of 100 μM using a robotic printer.

The binding specificity of four monoclonal antibodies (mAbs) targeting fucoidan, BAM1 to BAM4, was investigated. These antibodies are instrumental in marine research, allowing for the visualization of algae and diatom cell walls.[3,4,12] Furthermore, they aid in the environmental detection and quantification of fucoidan in seawater and sediments.[3,4,7] A current limitation of these antibodies is that their epitopes are not precisely defined.[12]

The microarray analysis uncovered distinct binding patterns for the mAbs BAM1, BAM3, BAM2, and BAM4. Notably, BAM1 and BAM3 exhibited a lack of binding to any fucoidan oligosaccharides on the array, suggesting a potential interaction with structural epitopes absent in the current library (Figure 5a). Conversely, mAb BAM4 demonstrated no binding to any fucoidan structures on the array but did display reproducible binding to a β-(1→3)-glucan tetrasaccharide **24** (SI Figure 15).

In the case of mAb BAM2, binding was observed to sulfated fucoidan oligosaccharides **11**, **9**, **13** and **14** (Figure 5a). Low level binding to glycan **11**, a monosaccharide with a di 3,4-*O*-sulfation pattern, was only observed at higher concentration of mAb BAM2 suggesting that this motif poorly represents the BAM2 epitope. While binding to α-(1→3)-fucoidan oligosaccharides (**9**, **13**, and **14**) with 4-*O*-sulfate esters and a terminal di 3,4-*O*-sulfation pattern provided more robust binding across a range of concentrations (SI Figure 15). This suggests that these oligosaccharides better represent the BAM2 epitope. The increasing relative fluorescence units (RFUs) of larger oligosaccharides, except for glycan **14**, suggest that larger synthetic glycans closely mimic polysaccharides.[14] The printing issue with glycan **14** may be due to lower

conjugation efficiency of larger oligosaccharides,[72] possibly because of their higher sulfate content.

Overall, the data presented here suggests a crucial component of the mAb BAM2 epitope is contained within the α-(1→3)-fucoidan oligosaccharides with 4-*O*-sulfate esters with terminal 3,4-di-*O*-sulfate groups.

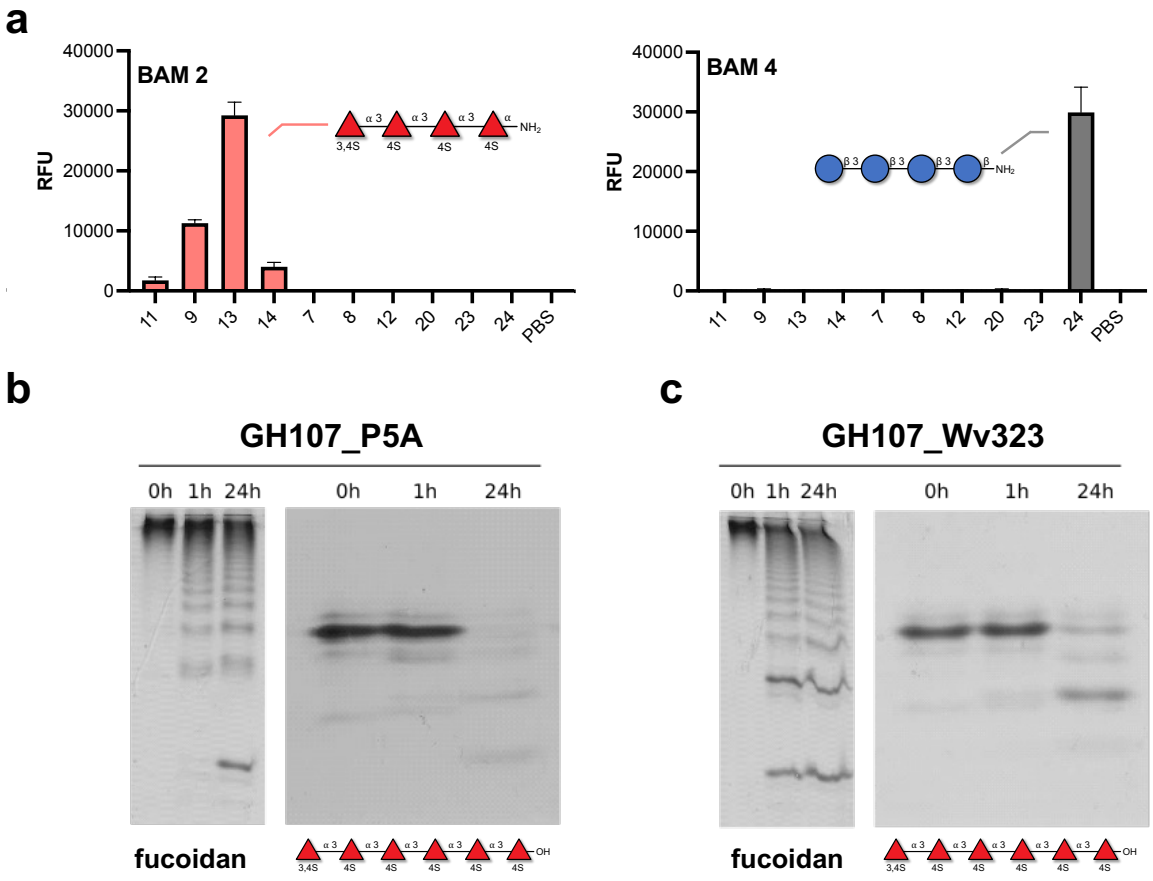

Figure 5. Synthetic fucoidans as tools for marine glycobiology. a Mapping the reactivity of BAM monoclonal antibodies with a fucoidan microarray. **b** Left gel shows activity of GH107_P5A on fucoidan from *L. hyperborea* by CPAGE. Right gel demonstrates activity of GH107_P5A on synthetic α-1,3 fucan oligosaccharide **10**. **c** Left gel is activity of GH107_Wv323 on fucoidan from *L. hyperborea* by CPAGE. Right gel shows activity of GH107_Wv323 on synthetic α-1,3 fucan oligosaccharide **10**. Enzyme incubations were complete at 1 μM for 0, 1 and 24 hours with each lane containing ~4 μg initial substrate. The products resulting from enzymatic degradation are separated according to size and degree of sulfation and visualized with Stains-All.

Binding of BAM2 to *Thalassiosira weissflogii* suggests the diatom synthesizes an α-(1→3)-fucoidan with 4-*O*-sulfate esters

The formation of sinking particles in the ocean promotes carbon sequestration, and microalgal polysaccharides are involved in this process. Recent findings, utilizing the fucoidan-specific monoclonal antibodies BAM1 and BAM2, have revealed that diatoms *Chaetoceros spp*. and *Thalassiosira weissflogii* produce fucose-containing sulfated polysaccharides (FCSP). These polysaccharides form particles that promote aggregation, sinking, and consequently, carbon sequestration.[4,73] FCSP is a broad term used to imply the presence of fucoidan-like structures, but does not refer to a particular structure.

Analysis of polysaccharide extracts from the diatom *Thalassiosira weissflogii* using microarrays suggested the presence distinct fucoidan that was reactive to BAM2 but not BAM1 (**Figure 6a**),[73] implying that diatom species synthesize diverse fucoidan structures. In this study, we mapped the specificity of the mAb BAM2, leading to the hypothesis that *T. weissflogii* produces a fucoidan with structural similarity to α-(1→3)-linked fucose oligosaccharides containing 4-O-sulfate esters, akin to those found in synthetic glycans. Microscopy analysis of diatom cells post-roller tank experiments, which were employed to induce aggregation, revealed the presence of the BAM2 fucoidan epitope surrounding the diatom cell aggregates.[73] Furthermore, here we demonstrate that individual diatom cells produce this fucoidan epitope and present it on their cell surface (**Figure 6b**).

The presence of structures akin to those found in brown algae, known for its carbon sequestration capacity, within a globally distributed diatom provides evidence that the synthesis of molecules known to sequester carbon is more prevalent than previously assumed. Detailed identification of glycans is crucial for obtaining a deeper understanding of the marine carbon cycle. In this process, structurally defined synthetic oligosaccharides serve as a missing link in various existing tools, including enzymatic, immunological, and spectroscopic methods.

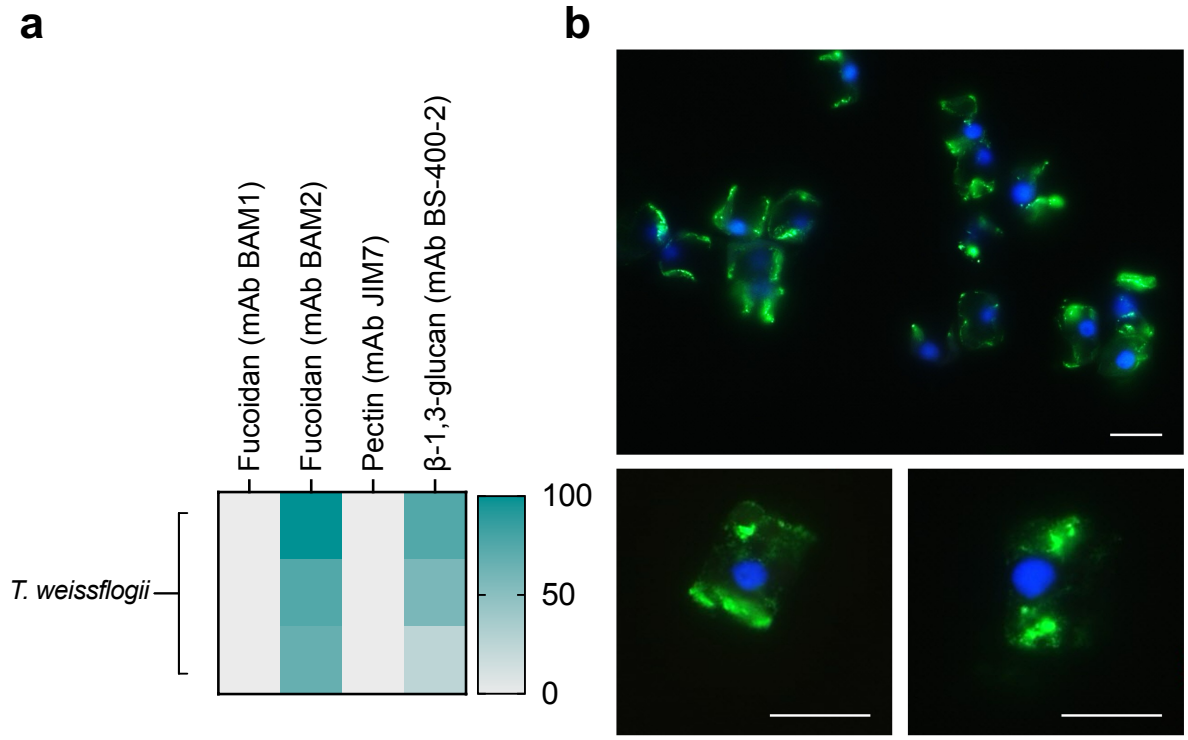

Figure 6. Binding of mAb BAM2 detects that *Thalassiosira weissflogii* produces fucoidan with α-(1→3)-fucose and 4-*O*-sulfate esters. a *T. weissflogii* water extracts were printed onto microarrays and those were probed with a panel of monoclonal antibodies (mAbs), each row represents a replicate. In addition to the anti-fucoidan BAM1 and BAM2, JIM7 (anti-pectin) and BS-400-2 (anti-β-1,3-glucan) were included as negative and positive controls, respectively. The heatmap shows normalized mAb binding intensity in the extraction triplicates. **b** Representative images showing that mAb BAM2 binds to *T. weissflogii* cells. Fluorescence microscopy images demonstrate BAM2 epitope is present on the diatom cell surfaces. α-1,3-linked fucoidan (green), DAPI (blue). Scale bars, 10 μm. Experiments were performed three times with similar results.

Conclusions

Automated glycan assembly (AGA) provides rapid access to fucoidan oligosaccharides, reaching lengths of up to 20-mers, with diverse branching patterns and up to 11 sulfate esters. Modulating the reactivity of building blocks was crucial for AGA of oligosaccharides, achieved by altering the thioglycoside aglycon from an alkyl to a less reactive aryl group. NMR experiments confirmed that these synthetic fucoidan oligosaccharides contain structural features found in brown algae. The synthetic oligosaccharide also enabled the characterization of two GH107 *endo*-fucoidanases from marine bacteria, with both enzymes capable of degrading α-(1→3)-linked fucoidan sulfated oligosaccharides. A fucoidan microarray of selected oligosaccharides was used to map the specificity of four monoclonal antibodies (mAbs) directed towards fucoidan. mAb BAM4 was discovered to have cross-reactivity towards a β-(1→3)-glucan curdlan structure, while mAb BAM2 had specificity for α-(1→3)-fucose oligosaccharides with 4-*O*-sulfate esters and terminal 3,4-di-*O*-sulfate groups. This enhanced understanding of mAb BAM2 specificity was used to uncover that this defined glycan motif is produced by a globally abundant diatom, *Thalassiosira weissflogii.* In summary, AGA offers a reproducible means to access well-defined fucoidan oligosaccharides. Synthetic glycans are tools to systematically investigate fucoidan's structure-function relationships in both carbon sequestration and its diverse bioactivities.

Acknowledgments

C.J.C. was funded by MSCA grant: MARINEGLYCAN (101029842). P.H.S acknowledges funding from the Max Planck Society.

Author contributions

C.J.C and P.L chemical synthesis. C.J.C and S.V.M glycan microarrays. M.S.J enzyme experiments. S.V.M microscopy. C.J.C, J.H.H, P.H.S writing original draft. All authors edited and approved the manuscript.

References

(1) Field, C. B.; Behrenfeld, M. J.; Randerson, J. T.; Falkowski, P. Primary Production of the Biosphere: Integrating Terrestrial and Oceanic Components. *Science* **1998**, *281* (5374), 237–240. https://doi.org/10.1126/SCIENCE.281.5374.237/SUPPL_FILE/982246E_THUMB.GIF.

(2) Bligh, M.; Nguyen, N.; Buck-Wiese, H.; Vidal-Melgosa, S.; Hehemann, J.-H. Structures and Functions of Algal Glycans Shape Their Capacity to Sequester Carbon in the Ocean. *Curr Opin Chem Biol* **2022**, *71*, 102204. https://doi.org/10.1016/J.CBPA.2022.102204.

(3) Buck-Wiese, H.; Andskog, M. A.; Nguyen, N. P.; Bligh, M.; Asmala, E.; Vidal-Melgosa, S.; Liebeke, M.; Gustafsson, C.; Hehemann, J. H. Fucoid Brown Algae Inject Fucoidan Carbon into the Ocean. *Proc Natl Acad Sci U S A* **2023**, *120* (1), e2210561119. https://doi.org/10.1073/PNAS.2210561119/SUPPL_FILE/PNAS.2210561119.SAPP.PDF.

(4) Vidal-Melgosa, S.; Sichert, A.; Francis, T. Ben; Bartosik, D.; Niggemann, J.; Wichels, A.; Willats, W. G. T.; Fuchs, B. M.; Teeling, H.; Becher, D.; Schweder, T.; Amann, R.; Hehemann, J. H. Diatom Fucan Polysaccharide Precipitates Carbon during Algal Blooms. *Nat Commun* **2021**, *12* (1). https://doi.org/10.1038/s41467-021-21009-6.

(5) Sichert, A.; Corzett, C. H.; Schechter, M. S.; Unfried, F.; Markert, S.; Becher, D.; Fernandez-Guerra, A.; Liebeke, M.; Schweder, T.; Polz, M. F.; Hehemann, J. H. Verrucomicrobia Use Hundreds of Enzymes to Digest the Algal Polysaccharide Fucoidan. *Nature Microbiology 2020 5:8* **2020**, *5* (8), 1026–1039. https://doi.org/10.1038/s41564-020-0720-2.

(6) Reintjes, G.; Heins, A.; Wang, C.; Amann, R. Abundance and Composition of Particles and Their Attached Microbiomes along an Atlantic Meridional Transect. *Front Mar Sci* **2023**, *10*, 1051510. https://doi.org/10.3389/FMARS.2023.1051510/BIBTEX.

(7) Vidal-Melgosa, S.; Lagator, M.; Sichert, A.; Priest, T.; Pätzold, J.; Hehemann, J.-H. Not Digested: Algal Glycans Move Carbon Dioxide into the Deep-Sea. *bioRxiv* **2022**, 2022.03.04.483023. https://doi.org/10.1101/2022.03.04.483023.

(8) Salmeán, A. A.; Willats, W. G. T.; Ribeiro, S.; Andersen, T. J.; Ellegaard, M. Over 100-Year Preservation and Temporal Fluctuations of Cell Wall Polysaccharides in Marine Sediments. *Front Plant Sci* **2022**, *13*, 785902. https://doi.org/10.3389/FPLS.2022.785902/BIBTEX.

(9) Priyan Shanura Fernando, I.; Kim, K. N.; Kim, D.; Jeon, Y. J. Algal Polysaccharides: Potential Bioactive Substances for Cosmeceutical Applications. *Crit Rev Biotechnol* **2019**, *39* (1), 99–113. https://doi.org/10.1080/07388551.2018.1503995.

(10) Fitton, J. H.; Stringer, D. N.; Karpiniec, S. S. Therapies from Fucoidan: An Update. *Mar Drugs* **2015**, *13* (9), 5920–5946. https://doi.org/10.3390/MD13095920.

(11) Crawford, C. J.; Seeberger, P. H. Advances in Glycoside and Oligosaccharide Synthesis. *Chem Soc Rev* **2023**, *52* (22), 7773–7801. https://doi.org/10.1039/D3CS00321C.

(12) Torode, T. A.; Marcus, S. E.; Jam, M.; Tonon, T.; Blackburn, R. S.; Hervé, C.; Knox, J. P. Monoclonal Antibodies Directed to Fucoidan Preparations from Brown Algae. *PLoS One* **2015**, *10* (2), e0118366. https://doi.org/10.1371/journal.pone.0118366.

(13) Geissner, A.; Reinhardt, A.; Rademacher, C.; Johannssen, T.; Monteiro, J.; Lepenies, B.; Thépaut, M.; Fieschi, F.; Mrázková, J.; Wimmerova, M.; Schuhmacher, F.; Götze, S.; Grünstein, D.; Guo, X.; Hahm, H. S.; Kandasamy, J.; Leonori, D.; Martin, C. E.; Parameswarappa, S. G.; Pasari, S.; Schlegel, M. K.; Tanaka, H.; Xiao, G.; Yang, Y.; Pereira, C. L.; Anish, C.; Seeberger, P. H. Microbe-Focused Glycan Array Screening Platform. *Proc Natl Acad Sci U S A* **2019**, *116* (6), 1958–1967. https://doi.org/10.1073/pnas.1800853116.

(14) Crawford, C. J.; Guazzelli, L.; McConnell, S. A.; McCabe, O.; d'Errico, C.; Greengo, S. D.; Wear, M. P.; Jedlicka, A. E.; Casadevall, A.; Oscarson, S. Synthetic Glycans Reveal Determinants of Antibody Functional Efficacy against a Fungal Pathogen. *ACS Infect Dis* **2024**, *10* (2), 475–488. https://doi.org/10.1021/acsinfecdis.3c00447.

(15) Becker, S.; Tebben, J.; Coffinet, S.; Wiltshire, K.; Iversen, M. H.; Harder, T.; Hinrichs, K. U.; Hehemann, J. H. Laminarin Is a Major Molecule in the Marine Carbon Cycle. *Proc Natl Acad Sci U S A* **2020**, *117* (12), 6599–6607. https://doi.org/10.1073/pnas.1917001117.

(16) Solanki, V.; Krüger, K.; Crawford, C. J.; Pardo-Vargas, A.; Danglad-Flores, J.; Hoang, K. L. M.; Klassen, L.; Abbott, D. W.; Seeberger, P. H.; Amann, R. I.; Teeling, H.; Hehemann, J.-H. Glycoside Hydrolase from the GH76 Family Indicates That Marine Salegentibacter Sp. Hel_I_6 Consumes Alpha-Mannan from Fungi. *ISME J* **2022**, *16* (7), 1818–1830. https://doi.org/10.1038/s41396-022-01223-w.

(17) Kelly, S. D.; Williams, D. M.; Nothof, J. T.; Kim, T.; Lowary, T. L.; Kimber, M. S.; Whitfield, C. The Biosynthetic Origin of Ribofuranose in Bacterial Polysaccharides. *Nature Chemical Biology 2022 18:5* **2022**, *18* (5), 530–537. https://doi.org/10.1038/s41589-022-01006-6.

(18) Delbianco, M.; Kononov, A.; Poveda, A.; Yu, Y.; Diercks, T.; Jiménez-Barbero, J.; Seeberger, P. H. Well-Defined Oligo- and Polysaccharides as Ideal Probes for Structural Studies. *J Am Chem Soc* **2018**, *140* (16), 5421–5426. https://doi.org/10.1021/JACS.8B00254.

(19) Canales, A.; Mallagaray, A.; Pérez-Castells, J.; Boos, I.; Unverzagt, C.; André, S.; Gabius, H. J.; Cañada, F. J.; Jiménez-Barbero, J. Breaking Pseudo-Symmetry in Multiantennary Complex N-Glycans Using Lanthanide-Binding Tags and NMR Pseudo-Contact Shifts. *Angew. Chem. Int. Ed.* **2013**, *52* (51), 13789–13793. https://doi.org/10.1002/anie.201307845.

(20) Hargett, A. A.; Azurmendi, H. F.; Crawford, C. J.; Wear, M. P.; Oscarson, S.; Casadevall, A.; Freedberg, D. I. The Structure of a C. Neoformans Polysaccharide Motif Recognized by Protective Antibodies: A Combined NMR and MD Study. *Proceedings of the National Academy of Sciences* **2024**, *121* (7), e2315733121. https://doi.org/10.1073/PNAS.2315733121.

(21) Joseph, A. A.; Pardo-Vargas, A.; Seeberger, P. H. Total Synthesis of Polysaccharides by Automated Glycan Assembly. *J Am Chem Soc* **2020**, *142* (19), 8561–8564. https://doi.org/10.1021/jacs.0c00751.

(22) Zhu, Y.; Delbianco, M.; Seeberger, P. H. Automated Assembly of Starch and Glycogen Polysaccharides. *J Am Chem Soc* **2021**, *143* (26), 9758–9768. https://doi.org/10.1021/JACS.1C02188/ASSET/IMAGES/LARGE/JA1C02188_0005.JPEG.

(23) Wang, L.; Overkleeft, H. S.; Van Der Marel, G. A.; Codée, J. D. C. Reagent Controlled Stereoselective Synthesis of α-Glucans. *J Am Chem Soc* **2018**, *140* (13), 4632–4638. https://doi.org/10.1021/jacs.8b00669.

(24) Lu, S. R.; Lai, Y. H.; Chen, J. H.; Liu, C. Y.; Mong, K. K. T. Dimethylformamide: An Unusual Glycosylation Modulator. *Angew. Chem. Int. Ed.* **2011**, *50* (32), 7315–7320. https://doi.org/10.1002/ANIE.201100076.

(25) Lemieux, R. U.; Hendriks, K. B.; Stick, R. V.; James, K. Halide Ion Catalyzed Glycosidation Reactions. Syntheses of α-Linked Disaccharides. *J Am Chem Soc* **1975**, *97* (14), 4056–4062. https://doi.org/10.1021/JA00847A032/ASSET/JA00847A032.FP.PNG_V03.

(26) Oscarson, S.; Sehgelmeble, F. W. A Novel β-Directing Fructofuranosyl Donor Concept. Stereospecific Synthesis of Sucrose. *J Am Chem Soc* **2000**, *122* (37), 8869–8872. https://doi.org/10.1021/JA001439U.

(27) Crich, D.; Sun, S. Formation of Beta-Mannopyranosides of Primary Alcohols Using the Sulfoxide Method. *J Org Chem* **1996**, *61* (14), 4506–4507. https://doi.org/10.1021/JO9606517.

(28) Hahm, H. S.; Broecker, F.; Kawasaki, F.; Mietzsch, M.; Heilbronn, R.; Fukuda, M.; Seeberger, P. H. Automated Glycan Assembly of Oligo-N-Acetyllactosamine and Keratan Sulfate Probes to Study Virus-Glycan Interactions. *Chem* **2017**, *2* (1), 114–124. https://doi.org/10.1016/j.chempr.2016.12.004.

(29) Tyrikos-Ergas, T.; Sletten, E. T.; Huang, J. Y.; Seeberger, P. H.; Delbianco, M. On Resin Synthesis of Sulfated Oligosaccharides. *Chem Sci* **2022**, *13* (7), 2115–2120. https://doi.org/10.1039/D1SC06063E.

(30) Tuck, O. T.; Sletten, E. T.; Danglad-Flores, J.; Seeberger, P. H. Towards a Systematic Understanding of the Influence of Temperature on Glycosylation Reactions. *Angew. Chem. Int. Ed.* **2022**, *61*, e202115433. https://doi.org/10.1002/ANIE.202115433.

(31) Zhang, Z.; Ollmann, I. R.; Ye, X. S.; Wischnat, R.; Baasov, T.; Wong, C. H. Programmable One-Pot Oligosaccharide Synthesis. *J Am Chem Soc* **1999**, *121* (4), 734–753. https://doi.org/10.1021/JA982232S.

(32) Lim, S. J.; Wan Aida, W. M.; Schiehser, S.; Rosenau, T.; Böhmdorfer, S. Structural Elucidation of Fucoidan from Cladosiphon Okamuranus (Okinawa Mozuku). *Food Chem* **2019**, *272*, 222–226. https://doi.org/10.1016/J.FOODCHEM.2018.08.034.

(33) Nagaoka, M.; Shibata, H.; Kimura-Takagi, I.; Hashimoto, S.; Kimura, K.; Makino, T.; Aiyama, R.; Ueyama, S.; Yokokura, T. Structural Study of

Fucoidan from Cladosiphon Okamuranus. *Glycoconj J* **1999**, *16* (1), 19–26. https://doi.org/10.1023/A:1006945618657/METRICS.

(34) Kopplin, G.; Rokstad, A. M.; Mélida, H.; Bulone, V.; Skjåk-Bræk, G.; Aachmann, F. L. Structural Characterization of Fucoidan from Laminaria Hyperborea: Assessment of Coagulation and Inflammatory Properties and Their Structure-Function Relationship. *ACS Appl Bio Mater* **2018**, *1* (6), 1880–1892. https://doi.org/10.1021/ACSABM.8B00436/ASSET/IMAGES/LARGE/MT-2018-00436R_0008.JPEG.

(35) Bilan, M. I.; Grachev, A. A.; Ustuzhanina, N. E.; Shashkov, A. S.; Nifantiev, N. E.; Usov, A. I. Structure of a Fucoidan from the Brown Seaweed Fucus Evanescens C.Ag. *Carbohydr Res* **2002**, *337* (8), 719–730. https://doi.org/10.1016/S0008-6215(02)00053-8.

(36) Jin, W.; Zhang, W.; Mitra, D.; McCandless, M. G.; Sharma, P.; Tandon, R.; Zhang, F.; Linhardt, R. J. The Structure-Activity Relationship of the Interactions of SARS-CoV-2 Spike Glycoproteins with Glucuronomannan and Sulfated Galactofucan from Saccharina Japonica. *Int J Biol Macromol* **2020**, *163*, 1649–1658. https://doi.org/10.1016/J.IJBIOMAC.2020.09.184.

(37) Koh, H. S. A.; Lu, J.; Zhou, W. Structure Characterization and Antioxidant Activity of Fucoidan Isolated from Undaria Pinnatifida Grown in New Zealand. *Carbohydr Polym* **2019**, *212*, 178–185. https://doi.org/10.1016/j.carbpol.2019.02.040.

(38) Deniaud-Bouët, E.; Hardouin, K.; Potin, P.; Kloareg, B.; Hervé, C. A Review about Brown Algal Cell Walls and Fucose-Containing Sulfated Polysaccharides: Cell Wall Context, Biomedical Properties and Key Research Challenges. *Carbohydr Polym* **2017**, *175*, 395–408. https://doi.org/10.1016/J.CARBPOL.2017.07.082.

(39) Patankar, M. S.; Oehninger, S.; Barnett, T.; Williams, R. L.; Clark, G. F. A Revised Structure for Fucoidan May Explain Some of Its Biological Activities. *Journal of Biological Chemistry* **1993**, *268* (29), 21770–21776. https://doi.org/10.1016/S0021-9258(20)80609-7.

(40) Behera, A.; Rai, D.; Kulkarni, S. S. Total Syntheses of Conjugation-Ready Trisaccharide Repeating Units of Pseudomonas Aeruginosa O11 and Staphylococcus Aureus Type 5 Capsular Polysaccharide for Vaccine

Development. *J Am Chem Soc* **2020**, *142* (1), 456–467. https://doi.org/10.1021/JACS.9B11309/SUPPL_FILE/JA9B11309_SI_001.PDF .

(41) Vinnitskiy, D. Z.; Krylov, V. B.; Ustyuzhanina, N. E.; Dmitrenok, A. S.; Nifantiev, N. E. The Synthesis of Heterosaccharides Related to the Fucoidan from Chordaria Flagelliformis Bearing an α-L-Fucofuranosyl Unit. *Org Biomol Chem* **2016**, *14* (2), 598–611. https://doi.org/10.1039/C5OB02040A.

(42) Kasai, A.; Arafuka, S.; Koshiba, N.; Takahashi, D.; Toshima, K. Systematic Synthesis of Low-Molecular Weight Fucoidan Derivatives and Their Effect on Cancer Cells. *Org Biomol Chem* **2015**, *13* (42), 10556–10568. https://doi.org/10.1039/C5OB01634G.

(43) Ye, X. S.; Wong, C. H. Anomeric Reactivity-Based One-Pot Oligosaccharide Synthesis: A Rapid Route to Oligosaccharide Libraries. *Journal of Organic Chemistry* **2000**, *65* (8), 2410–2431. https://doi.org/10.1021/JO991558W.

(44) Danglad-Flores, J.; Leichnitz, S.; Sletten, E. T.; Abragam Joseph, A.; Bienert, K.; Le Mai Hoang, K.; Seeberger, P. H. Microwave-Assisted Automated Glycan Assembly. *J Am Chem Soc* **2021**, *143* (23), 8893–8901. https://doi.org/10.1021/JACS.1C03851/SUPPL_FILE/JA1C03851_SI_001.PDF .

(45) Lahmann, M.; Oscarson, S. Investigation of the Reactivity Difference between Thioglycoside Donors with Variant Aglycon Parts. *Can J Chem* **2002**, *80* (8), 889–893. https://doi.org/10.1139/v02-101.

(46) Le Mai Hoang, K.; Pardo-Vargas, A.; Zhu, Y.; Yu, Y.; Loria, M.; Delbianco, M.; Seeberger, P. H. Traceless Photolabile Linker Expedites the Chemical Synthesis of Complex Oligosaccharides by Automated Glycan Assembly. *J Am Chem Soc* **2019**, *141* (22), 9079–9086. https://doi.org/10.1021/JACS.9B03769.

(47) Calabro, A.; Midura, R.; Wang, A.; West, L.; Plaas, A.; Hascall, V. C. Fluorophore-Assisted Carbohydrate Electrophoresis (FACE) of Glycosaminoglycans. *Osteoarthritis Cartilage* **2001**, *9* (SUPPL. A), S16–S22. https://doi.org/10.1053/JOCA.2001.0439.

(48) Yu, Y.; Kononov, A.; Delbianco, M.; Seeberger, P. H. A Capping Step During Automated Glycan Assembly Enables Access to Complex Glycans in High Yield. *Chemistry - A European Journal* **2018**, *24* (23), 6075–6078. https://doi.org/10.1002/chem.201801023.

(49) Tyrikos-Ergas, T.; Bordoni, V.; Fittolani, G.; Chaube, M. A.; Grafmüller, A.; Seeberger, P. H.; Delbianco, M. Systematic Structural Characterization of Chitooligosaccharides Enabled by Automated Glycan Assembly. *Chemistry – A European Journal* **2021**, *27* (7), 2321–2325. https://doi.org/10.1002/CHEM.202005228.

(50) Eller, S.; Collot, M.; Yin, J.; Hahm, H. S.; Seeberger, P. H. Automated Solid-Phase Synthesis of Chondroitin Sulfate Glycosaminoglycans. *Angew. Chem. Int. Ed.* **2013**, *52* (22), 5858–5861. https://doi.org/10.1002/anie.201210132.

(51) Crawford, C. J.; Qiao, Y.; Liu, Y.; Huang, D.; Yan, W.; Seeberger, P. H.; Oscarson, S.; Chen, S. Defining the Qualities of High-Quality Palladium on Carbon Catalysts for Hydrogenolysis. *Org Process Res Dev* **2021**, *25* (7), 1573–1578. https://doi.org/10.1021/acs.oprd.0c00536.

(52) Schumann, B.; Parameswarappa, S. G.; Lisboa, M. P.; Kottari, N.; Guidetti, F.; Pereira, C. L.; Seeberger, P. H. Nucleophile-Directed Stereocontrol Over Glycosylations Using Geminal-Difluorinated Nucleophiles. *Angewandte Chemie International Edition* **2016**, *55* (46), 14431–14434. https://doi.org/10.1002/ANIE.201606774.

(53) Chopra, P.; Joshi, A.; Wu, J.; Lu, W.; Yadavalli, T.; Wolfert, M. A.; Shukla, D.; Zaia, J.; Boons, G. J. The 3-O-Sulfation of Heparan Sulfate Modulates Protein Binding and Lyase Degradation. *Proc Natl Acad Sci U S A* **2021**, *118* (3), e2012935118. https://doi.org/10.1073/PNAS.2012935118/SUPPL_FILE/PNAS.2012935118.SAPP.PDF.

(54) Sankarayanarayanan, N. V.; Strebel, T. R.; Boothello, R. S.; Sheerin, K.; Raghuraman, A.; Sallas, F.; Mosier, P. D.; Watermeyer, N. D.; Oscarson, S.; Desai, U. R. A Hexasaccharide Containing Rare 2-O-Sulfate-Glucuronic Acid Residues Selectively Activates Heparin Cofactor II. *Angewandte Chemie International Edition* **2017**, *56* (9), 2312–2317. https://doi.org/10.1002/ANIE.201609541.

(55) de Paz, J. L.; Moseman, E. A.; Noti, C.; Polito, L.; von Andrian, U. H.; Seeberger, P. H. Profiling Heparin - Chemokine Interactions Using Synthetic Tools. *ACS Chem Biol* **2007**, *2* (11), 735–744. https://doi.org/10.1021/CB700159M/ASSET/IMAGES/LARGE/CB-2007-00159M_0006.JPEG.

(56) Chhabra, M.; Wimmer, N.; He, Q. Q.; Ferro, V. Development of Improved Synthetic Routes to Pixatimod (PG545), a Sulfated Oligosaccharide-Steroid Conjugate. *Bioconjug Chem* **2021**, *32* (11), 2420–2431. https://doi.org/10.1021/ACS.BIOCONJCHEM.1C00453.

(57) Chen, L.; Lee, S.; Renner, M.; Tian, Q.; Nayyar, N. A Simple Modification to Prevent Side Reactions in Swern-Type Oxidations Using Py·SO3. *Org Process Res Dev* **2006**, *10* (1), 163–164. https://doi.org/10.1021/OP0502203/ASSET/IMAGES/LARGE/OP0502203H00001.JPEG.

(58) Santini, R.; Griffith, M. C.; Qi, M. A Measure of Solvent Effects on Swelling of Resins for Solid Phase Organic Synthesis. *Tetrahedron Lett* **1998**, *39* (49), 8951–8954. https://doi.org/10.1016/S0040-4039(98)02069-3.

(59) Sarin, V. K.; Kent, S. B. H.; Merrifield, R. B. Properties of Swollen Polymer Networks. Solvation and Swelling of Peptide-Containing Resins in Solid-Phase Peptide Synthesis. *J Am Chem Soc* **1980**, *102* (17), 5463–5470. https://doi.org/10.1021/JA00537A006/ASSET/JA00537A006.FP.PNG_V03.

(60) Bakhatan, Y.; Alshanski, I.; Grunhaus, D.; Hurevich, M. The Breaking Beads Approach for Photocleavage from Solid Support. *Org Biomol Chem* **2020**, *18* (22), 4183–4188. https://doi.org/10.1039/D0OB00821D.

(61) Teschers, C. S.; Gilmour, R. Flow Photocleavage for Automated Glycan Assembly (AGA). *Org Process Res Dev* **2020**, *24* (10), 2234–2239. https://doi.org/10.1021/ACS.OPRD.0C00286/ASSET/IMAGES/MEDIUM/OP0C00286_M002.GIF.

(62) Jin, W.; Lu, C.; Zhu, Y.; Zhao, J.; Zhang, W.; Wang, L.; Linhardt, R. J.; Wang, C.; Zhang, F. Fucoidans Inhibited Tau Interaction and Cellular Uptake. *Carbohydr Polym* **2023**, *299*, 120176. https://doi.org/10.1016/J.CARBPOL.2022.120176.

(63) Bartetzko, M. P.; Schuhmacher, F.; Hahm, H. S.; Seeberger, P. H.; Pfrengle, F. Automated Glycan Assembly of Oligosaccharides Related to Arabinogalactan Proteins. *Org Lett* **2015**, *17* (17), 4344–4347. https://doi.org/10.1021/ACS.ORGLETT.5B02185/SUPPL_FILE/OL5B02185_SI_001.PDF.

(64) Orellana, L. H.; Francis, T. Ben; Ferraro, M.; Hehemann, J. H.; Fuchs, B. M.; Amann, R. I. Verrucomicrobiota Are Specialist Consumers of Sulfated Methyl

Pentoses during Diatom Blooms. *The ISME Journal 2021 16:3* **2021**, *16* (3), 630–641. https://doi.org/10.1038/s41396-021-01105-7.

(65) Becker, S.; Scheffel, A.; Polz, M. F.; Hehemann, J. H. Accurate Quantification of Laminarin in Marine Organic Matter with Enzymes from Marine Microbes. *Appl Environ Microbiol* **2017**, *83* (9). https://doi.org/10.1128/AEM.03389-16.

(66) Steinke, N.; Vidal-Melgosa, S.; Schultz-Johansen, M.; Hehemann, J. Biocatalytic Quantification of A-glucan in Marine Particulate Organic Matter. *Microbiologyopen* **2022**, *11* (3), e1289. https://doi.org/10.1002/mbo3.1289.

(67) Drula, E.; Garron, M. L.; Dogan, S.; Lombard, V.; Henrissat, B.; Terrapon, N. The Carbohydrate-Active Enzyme Database: Functions and Literature. *Nucleic Acids Res* **2022**, *50* (D1), D571–D577. https://doi.org/10.1093/NAR/GKAB1045.

(68) Vickers, C.; Liu, F.; Abe, K.; Salama-Alber, O.; Jenkins, M.; Springate, C. M. K.; Burke, J. E.; Withers, S. G.; Boraston, A. B. Endo-Fucoidan Hydrolases from Glycoside Hydrolase Family 107 (GH107) Display Structural and Mechanistic Similarities to α-l-Fucosidases from GH29. *J Biol Chem* **2018**, *293* (47), 18296. https://doi.org/10.1074/JBC.RA118.005134.

(69) Mikkelsen, M. D.; Tran, V. H. N.; Meier, S.; Nguyen, T. T.; Holck, J.; Cao, H. T. T.; Van, T. T. T.; Thinh, P. D.; Meyer, A. S.; Morth, J. P. Structural and Functional Characterization of the Novel Endo-α(1,4)-Fucoidanase Mef1 from the Marine Bacterium Muricauda Eckloniae. *Acta Crystallogr D Struct Biol* **2023**, *79* (Pt 11), 1026–1043. https://doi.org/10.1107/S2059798323008732.

(70) Tran, V. H. N.; Nguyen, T. T.; Meier, S.; Holck, J.; Cao, H. T. T.; Van, T. T. T.; Meyer, A. S.; Mikkelsen, M. D. The Endo-α(1,3)-Fucoidanase Mef2 Releases Uniquely Branched Oligosaccharides from Saccharina Latissima Fucoidans. *Mar Drugs* **2022**, *20* (5). https://doi.org/10.3390/MD20050305.

(71) Alejandre-Colomo, C.; Francis, B.; Viver, T.; Harder, J.; Fuchs, B. M.; Rossello-Mora, R.; Amann, R. Cultivable Winogradskyella Species Are Genomically Distinct from the Sympatric Abundant Candidate Species. *ISME Communications 2021 1:1* **2021**, *1* (1), 1–10. https://doi.org/10.1038/s43705-021-00052-w.

(72) Ruprecht, C.; Geissner, A.; Seeberger, P. H.; Pfrengle, F. Practical Considerations for Printing High-Density Glycan Microarrays to Study Weak

Carbohydrate-Protein Interactions. *Carbohydr Res* **2019**, *481*, 31–35. https://doi.org/10.1016/J.CARRES.2019.06.006.

(73) Huang, G.; Vidal-Melgosa, S.; Sichert, A.; Becker, S.; Fang, Y.; Niggemann, J.; Iversen, M. H.; Cao, Y.; Hehemann, J. H. Secretion of Sulfated Fucans by Diatoms May Contribute to Marine Aggregate Formation. *Limnol Oceanogr* **2021**, *66* (10), 3768–3782. https://doi.org/10.1002/LNO.11917.